

# Cryogenic milling for the fabrication of high $J_c$ MgB<sub>2</sub> bulk superconductors

D. N. Kim<sup>a,b</sup>, M. O. Kang<sup>a,b</sup>, B.-H. Jun<sup>b</sup>, C.-J. Kim<sup>\*b</sup>, and H. W. Park<sup>\*a</sup>

<sup>a</sup> Korea University of Technology and Education, Cheon-an, Korea

<sup>b</sup> Korea Atomic Energy Research Institute, Daejeon, Korea

(Received 6 May 2017; revised or reviewed 15 June 2017; accepted 16 June 2017)

## Abstract

Cryogenic milling which is a combined process of low-temperature treatment and mechanical milling was applied to fabricate high critical current density ( $J_c$ ) MgB<sub>2</sub> bulk superconductors. Liquid nitrogen was used as a coolant, and no solvent or lubricant was used. Spherical Mg (6-12  $\mu\text{m}$ , 99.9 % purity) and plate-like B powder ( $\sim 1 \mu\text{m}$ , 97 % purity) were milled simultaneously for various time periods (0, 2, 4, 6 h) at a rotating speed of 500 rpm using ZrO<sub>2</sub> balls. The (Mg+2B) powders milled were pressed into pellets and heat-treated at 700°C for 1 h in flowing argon. The use of cryomilled powders as raw materials promoted the formation reaction of superconducting MgB<sub>2</sub>, reduced the grain size of MgB<sub>2</sub>, and suppressed the formation of impurity MgO. The superconducting critical temperature ( $T_c$ ) of MgB<sub>2</sub> was not influenced as the milling time ( $t$ ) increased up to 6 h. Meanwhile, the critical current density ( $J_c$ ) of MgB<sub>2</sub> increased significantly when  $t$  increased to 4 h. When  $t$  increased further to 6 h, however,  $J_c$  decreased. The  $J_c$  enhancement of MgB<sub>2</sub> by cryogenic milling is attributed to the formation of the fine grain MgB<sub>2</sub> and a suppression of the MgO formation.

**Keywords:** MgB<sub>2</sub>, Cryogenic milling, Milling time, Critical current density, Grain refinement

## 1. INTRODUCTION

Because of the high superconducting critical temperature ( $T_c$ ) of 39 K of MgB<sub>2</sub> [1], MgB<sub>2</sub> is considered as a promising material that can replace the convention NbTi superconducting material. Compared to NbTi, which uses expensive liquid helium as a coolant, MgB<sub>2</sub> can be cooled without using liquid helium. Superconducting magnets operating at 20 K can be made using MgB<sub>2</sub>. To use MgB<sub>2</sub> in practical applications, MgB<sub>2</sub> should be fabricated into a wire form. A powder-in-tube (PIT) method is widely used to manufacture MgB<sub>2</sub> superconducting wires with a high critical current density ( $J_c$ ) [2-6]. In the PIT process magnesium (Mg) and boron (B) or MgB<sub>2</sub> powders are put in a metal or alloy tube and the tube is mechanically drawn into a wire form. After the wire forming process, the metal/alloy sheathed MgB<sub>2</sub> wire is heat-treated to form a MgB<sub>2</sub> superconducting phase or to connect the MgB<sub>2</sub> grains together [4, 5].

During the heat treatment MgB<sub>2</sub> forms through a solid or a liquid state reaction of Mg and B powders [7, 8]. The melting point (m. p.) of B is as high as 2200°C [9], whereas that of Mg is as low as 650°C [10]. The diffusion of B is relatively very slow compared to that of Mg. Therefore, the fast diffusion of Mg controls the formation reaction of MgB<sub>2</sub>, whereas B serves as a nucleation site of MgB<sub>2</sub>. When a powder mixture of Mg and B is heat-treated at temperatures below the m. p. of Mg, MgB<sub>2</sub> forms through the solid state reaction of Mg and B [8]. When the two raw powders are heat-treated at temperatures higher than 650°C,

the formation reaction of MgB<sub>2</sub> proceeds through the melt-solid (Mg-B) reaction process [8, 11].

$J_c$  of MgB<sub>2</sub> depends on the microstructure of the material, such as the lattice strains, carbon doping, microdefects and grain size of MgB<sub>2</sub> [2, 5, 6]. The smaller the grain size, the higher the  $J_c$  in the magnetic fields [8]. This is because the grain boundaries of MgB<sub>2</sub> effectively act as flux pinning centers that trap the external magnetic field. Therefore, the grain structure of MgB<sub>2</sub> should be controlled by reducing the size of the raw powders [8].

Mechanical milling has been used to reduce the size of raw powders of MgB<sub>2</sub> [12-14]. The size of both Mg and B powders can be reduced through mechanical milling. Because Mg is highly oxidative, however, there is a risk of an explosion during the milling of Mg powder. For this reason, only B powder is milled, and the milled B powder is mixed with non-milled Mg powder by hand [12]. If the Mg and B powders can be crushed and mixed simultaneously, a fine powder mixture with an improve homogeneity can be made, in which further increases of  $J_c$  of MgB<sub>2</sub> can be expected.

A method suitable for reducing the size of B and Mg powders simultaneously and safely is cryogenic milling (hereafter, cryomilling). Cryogenic milling is a combined process of mechanical milling and low-temperature treatment [15]. In the cryomilling process liquid nitrogen (LN<sub>2</sub>) or liquid argon is used as a refrigerant to prevent oxidation of the targeting materials and to brittle the raw materials, thereby maximizing the milling effect.

In this study, cryomilling was attempted to reduce the size of Mg and B powders and to mix the two powders uniformly. The effects of the milling time on the formation

\*Corresponding authors: hwpark@koreatech.ac.kr, and cjkim2@kaeri.re.kr

of MgB<sub>2</sub> and the superconducting properties of the MgB<sub>2</sub> bulk superconductors were studied.

## 2. EXPERIMENT PROCEDURE

Fig. 1 (a) shows the milling machine used for the mixing and milling of Mg and B powders. A commercial attrition milling device was modified to use LN<sub>2</sub> as a coolant. LN<sub>2</sub> supply lines from a liquid nitrogen chamber to a milling chamber were made, and thus LN<sub>2</sub> can flow into the milling chamber. A thermocouple was attached at the outer wall of the chamber to monitor the temperature of the milling chamber. When the milling chamber was filled with LN<sub>2</sub>, the temperature of the outer wall measured using the thermocouple was about 150 K.

Crushing or mixing objects (Mg and 2B powders) were put in a milling chamber together with ZrO<sub>2</sub> balls (a milling media) with a diameter of 3 mm. The weight ratio of the ZrO<sub>2</sub> balls and the (Mg+2B) powder was 5:1. Mg powder of 5-10 μm in size and B powder with a size of ~1 μm were used as raw powders.

Fig. 2 shows Mg and B powders used as the raw materials of this study. As can be seen in Fig. 2(a), many tiny Mg particles are attached on the surfaces of the large spherical Mg powders. The B powder is plate-like in shape and relatively smaller than the Mg powder. A mixture of Mg and B powders, and ZrO<sub>2</sub> balls, were put together in a steel jar filled with liquid nitrogen. No organic solvent or

lubricant was used. To understand the optimum milling condition, Mg and B powders were milled separately with variations in rotating speed of 100-500 rpm and milling time ( $t$ ). Based on the results obtained from the preliminary milling experiment, the rotating speed was determined as 500 rpm. The powder mixtures of (Mg+2B) were milled for 0, 2, 4, and 6 h at 500 rpm, respectively. After milling, the milled powder was dried at 50°C in a vacuum oven.

Fig. 3 shows scanning electron micrographs (SEM) of the (Mg+2B) powders milled for (a) 0 h, (b) 2 h, (c) 4 h, and (d) 6 h. In this figure, the large spherical particles are Mg powders, whereas the small particles are B powders and fragments formed by milling. As  $t$  increases, the number of small irregular shaped powders increases. However, many large spherical Mg powders are still observed as unbroken. It is believed that when  $t$  is short, only the surfaces of the Mg powders are dominantly grounded. When  $t$  increased to 6 h, some of the Mg powders are found to be partly broken into smaller pieces (see Fig. 3(d)). As a result of the fracture of Mg powders, the shape of the Mg powder is no longer spherical. Not clearly observed here, B powders are thought to also be crushed into smaller powders by milling, depending on the milling time.

The (Mg +2B) powders milled for 0-6 h were uniaxially pressed into pellets at a pressure of 3 tons in a steel mold with a diameter of 20 mm. The pellets were encapsulated with a Ti tube to prevent Mg oxidation during heat treatment. The Ti-encapsulated pellets were placed at the center of a tubular furnace, heated to 700°C at a heating rate of 100°C/h, held at this temperature for 1 h and then furnace-cooled. During the heat treatment, argon gas was flowed into a tubular furnace. The heat treatment cycles applied to the pellets is the same as that carried out in the previous work [5].

After the heat treatment, the pellets were taken out of the Ti tube. The apparent density of the MgB<sub>2</sub> pellets was calculated by measuring the diameter, weight and thickness of the pellets before and after the heat treatment.

Some of the pellets were crushed into a powder form to analyze the phases formed in the pellets. An X-ray diffraction (XRD) analysis using a CuK<sub>α</sub> target was carried

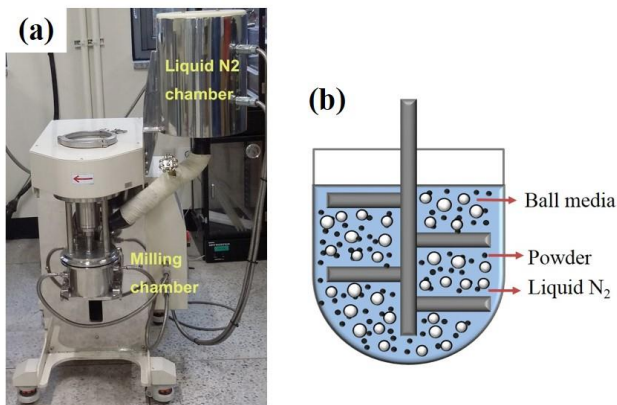


Fig. 1. Photo of (a) cryomilling device and (b) schematic of a milling chamber using LN<sub>2</sub> as a refrigerant.

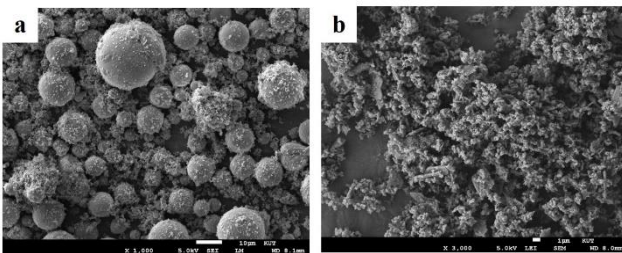


Fig. 2. Scanning electron micrographs of (a) Mg and (b) B powders used as raw materials.

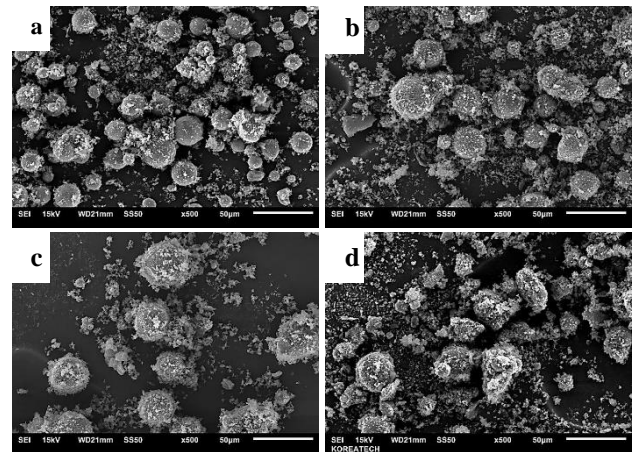


Fig. 3. SEM micrographs of a powder mixture of (Mg+2B) milled for (a) 0 h, (b) 2 h, (c) 4 h, and (d) 6 h.

out for scan angles of  $2\theta=20-80$  degrees. The grain size of  $\text{MgB}_2$  was calculated from the formula  $T=0.9\lambda/BCOS\theta$  [16] using the FWHM (Full width at half maximum) data of the  $\text{MgB}_2$  peaks, where  $T$  is the grain (crystallite) size of  $\text{MgB}_2$ ,  $\lambda$  is the wavelength of the target used,  $B$  is the half width of the peak, and  $\theta$  is the Bragg angle of an incident beam.

For the measurement of  $T_c$  and  $J_c$  of  $\text{MgB}_2$ , rectangular specimens with approximate dimensions of  $3\times 3\times 2$  mm were cut from the heat-treated pellets using a diamond saw. The temperature dependence of magnetization ( $M-T$ ) was measured using a magnetic property measurement system (MPMS) to understand the superconducting transition temperatures of  $\text{MgB}_2$ . The magnetic field dependence of the magnetization ( $M-H$ ) of  $\text{MgB}_2$  was measured with a maximum magnetic field of 5 Tesla (T).  $J_c$ s at 5 K and 20 K were calculated using an extended version of Bean's critical model [17] of eq. (1),

$$J_c = 20\Delta M/a(1-a/3b) \quad (1)$$

where  $\Delta M$  is the magnetization difference ( $M(\text{decreasing field region})-M(\text{increasing field region})$ ) at a constant magnetic field, and  $a$  and  $b$  are parameters regarding the sample dimensions.

### 3. RESULTS AND DISCUSSION

Fig. 4 shows a histogram of the apparent density before and after the heat treatment as a function of milling time ( $t$ ). The apparent density of the  $\text{MgB}_2$  pellets before the heat treatment was  $1.35-1.47 \text{ g/cm}^3$ . After the heat treatment it was reduced to  $1.23-1.27 \text{ g/cm}^3$ . The density reduction after the heat treatment was approximately 12-20 %. The density decrease is attributed to the increase in diameter and thickness, as well as the weight loss of the  $\text{MgB}_2$  pellets. In other words, it is due to the vaporization of Mg and the volume increase (so-called pellet expansion [18,19]) from the out-growth of plate-like  $\text{MgB}_2$  grains during the powder reaction of ( $\text{Mg}+2\text{B}=\text{MgB}_2$ ), which has been reported in *in situ* reaction processing using Mg and B as raw materials [8,20], and in the reaction processed BiPbSrCaCuO oxides [18,19].

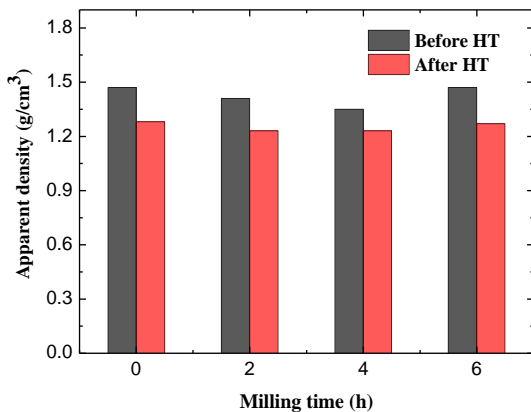


Fig. 4. Histogram of apparent densities of  $\text{MgB}_2$  pellets before/after heat treatment as a function of milling time.

TABLE I  
VARIATION IN APPARENT DENSITY OF  $\text{MgB}_2$  PELLETS AS A FUNCTION OF MILLING TIME.

Milling time (h)	Density before	Density after
	HT(g/cm³)	HT(g/cm³)
0	1.44	1.28
2	1.41	1.23
4	1.35	1.23
6	1.47	1.27

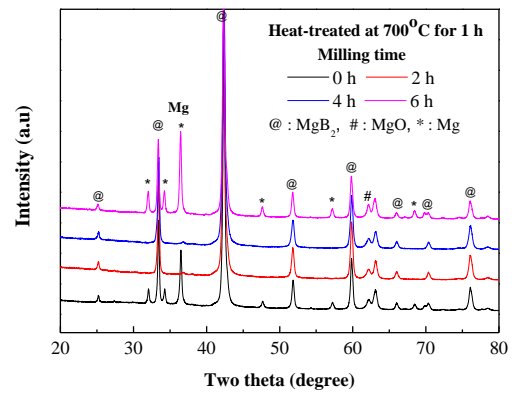


Fig. 5. Powder X-ray diffraction patterns of the pellets heat-treated using non-milled and ( $\text{Mg}+2\text{B}$ ) powders milled for 2-6 h.

Owing to the pellet expansion the apparent density of  $\text{MgB}_2$  after heat treatment decreased down to 50 % of the theoretical density ( $2.57 \text{ g/cm}^3$  [21]). The density decrease in the powder reaction processed  $\text{MgB}_2$  is an important issue to be solved for the enhancement of  $J_c$  of  $\text{MgB}_2$ . The variations in apparent density of the  $\text{MgB}_2$  pellets before/after heat treatment are summarized in TABLE I.

Fig. 5 shows the powder XRD patterns of the  $\text{MgB}_2$  pellets prepared using non-milled powder and ( $\text{Mg}+2\text{B}$ ) powders milled for 2-6 h. As can be seen in the figure, the main formed phase of all pellets is  $\text{MgB}_2$ . In the case of a pellet prepared using the non-milled powder, the diffraction peak of Mg is clearly observed near  $2\theta=37$  degrees, which indicates the incomplete formation reaction of  $\text{MgB}_2$ . Meanwhile, the Mg peak is not observed in the pellets prepared using powders milled for 2 and 4 h. Most of the peaks of the pellets belong to  $\text{MgB}_2$ . This result indicates that the formation reaction of  $\text{MgB}_2$  was promoted when the milled powders were used as raw materials. However, as  $t$  increases to 6 h, the Mg peaks appears in the XRD pattern again. The prolonged milling can produce very fine Mg or B powders with a high specific surface area. When the surface area of the Mg and B powders is large, the powders has a strong adsorption capability, and thus the impurity species included in air may be easily incorporated with the powders and suppress the formation reaction of  $\text{MgB}_2$ . Further systematic study is needed to understand the exact reason why the formation reaction of  $\text{MgB}_2$  was suppressed when using the

prolonged milled powder.

In addition to the formation characteristics of MgB<sub>2</sub>, the formation of MgO should be mentioned. The formation of MgO has been consistently reported in powder reaction processed MgB<sub>2</sub> [22, 23]. Although an inert argon gas was used to prevent the oxidation of Mg, MgO was formed through the magnesium-oxygen reaction [22]. The oxidation of Mg in the powder reaction process looks inevitable. The XRD patterns of the heat-treated MgB<sub>2</sub> pellets of Fig. 5 already showed that the amount of MgO formed in the heat-treated pellets of this study was small. This is comparable to the results (the formation of a large amount of MgO) of MgB<sub>2</sub> prepared with B powder milled using organic solvents [12, 13]. The use of LN<sub>2</sub> as a solvent (or lubricant) instead of organic C<sub>x</sub>H<sub>y</sub>O<sub>z</sub> solvents containing oxygen (for example, the chemical formula of acetone and alcohol are CH<sub>3</sub>COCH<sub>3</sub> and RCH<sub>2</sub>OH, respectively) seems to make it difficult for oxygen to be incorporated with the milled Mg powders.

Fig. 6 shows the variation of grain size of MgB<sub>2</sub> with  $t$ . The grain size of MgB<sub>2</sub> prepared using the non-milled (Mg+2B) powder is 90.5 nm. The grain size decreases to 77, 70 and 53 nm, respectively, as  $t$  increases to 2, 4 and 6 h. The decrease in grain size of MgB<sub>2</sub> with increasing  $t$  has been reported in MgB<sub>2</sub> using glycerin treated boron and ball-milled B powder [14]. The optimum condition for the formation of high  $J_c$  MgB<sub>2</sub> was 2 h of milling at 200 rpm. The grain refinement of MgB<sub>2</sub> by milling is thought to be a result of the increased number of nucleation sites (B powders) for MgB<sub>2</sub> by milling. It can thus be said that the simultaneous milling of the two powders (Mg+2B) of this study not only facilitated the diffusion of Mg for the formation of MgB<sub>2</sub> but also provided more nucleation sites for MgB<sub>2</sub>.

Fig. 7 shows the normalized  $M$ - $T$  curves of the heat-treated MgB<sub>2</sub> pellets using the non-milled and (Mg+2B) milled powders for 2-6 h. The superconducting onset temperature ( $T_{c,onset}$ ) of MgB<sub>2</sub> without milling is 37 K and  $T_{c,onset}$ s of MgB<sub>2</sub> with  $t=2$  h,  $t=4$  h and  $t=6$  h are 37.5 K, 37.5 K and 37 K, respectively. There is no significant difference in  $T_{c,onset}$  among the MgB<sub>2</sub> pellets. The superconducting transition width

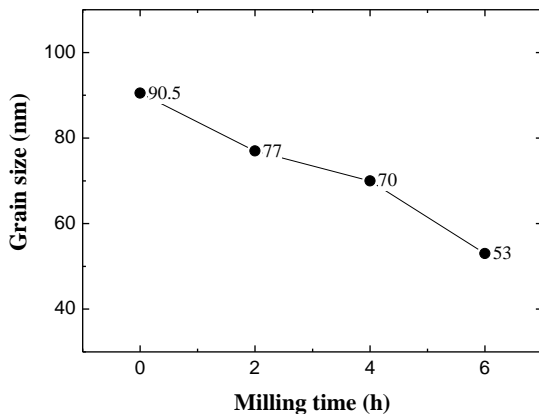


Fig. 6. Variation in grain size of MgB<sub>2</sub> as a function of milling time.

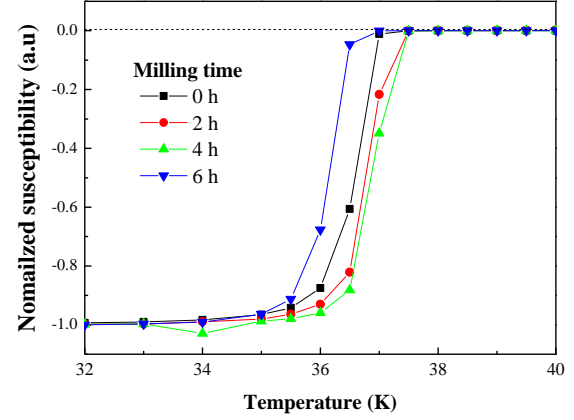


Fig. 7. Normalized  $M$ - $T$  curves of MgB<sub>2</sub> prepared using the non-milled and (Mg+2B) powders milled for 2-6 h.

TABLE II  
SUPERCONDUCTING TEMPERATURES AS A FUNCTION OF MILLING TIME OF MgB<sub>2</sub> PREPARED USING THE MILLED POWDERS.

Milling time (h)	0	2	4	6
$T_{c,onset}$ (K)	37	37.5	37.5	37
$T_{c,mid}$ (K)	36.2	36.8	36.9	36.6
$\Delta T_c$ (K)	1.5	2	2	2

( $\Delta T_c = T_{c,onset} - T_{c,0}$ ) of MgB<sub>2</sub> with  $t=0$  h is 1.5 K and  $\Delta T_c$  of other MgB<sub>2</sub> pellets is 2 K. The effect of cryomilling on the  $T_{c,onset}$  of MgB<sub>2</sub> seems to be relatively small compared with the conventional milling process [14]. The  $J_c$  of MgB<sub>2</sub> was reported to be dependent on the type of an organic solvent used [14]. When the organic liquid was used as a solvent, carbon was incorporated with the milled powder and formed Mg(B<sub>1-x</sub>C<sub>x</sub>)<sub>2</sub>, or formed MgO, thereby reducing  $T_c$  of MgB<sub>2</sub> [5, 12-14]. Compared to the milling using organic solvents, there was no possibility of the carbon incorporation in the cryomilling. The superconducting temperatures of MgB<sub>2</sub> pellets prepared using cryomilled powders are summarized in TABLE II.

Fig. 8 shows the  $J_c$ - $B$  curves at 5 K and 20 K of MgB<sub>2</sub> prepared using the non-milled and (Mg+2B) powder milled for 2-6 h. As can be seen in the  $J_c$ - $B$  curves,  $J_c$  of MgB<sub>2</sub> prepared using the non-milled powder is the lowest in all measured magnetic fields. As  $t$  increases to 2 and 4 h,  $J_c$  increases. The value of  $J_c$  at 5 K and 20 K, with 2 T of MgB<sub>2</sub> prepared using milled powder for 4 h was  $4.49 \times 10^4$  A/cm<sup>2</sup> and  $7.91 \times 10^3$  A/cm<sup>2</sup>, respectively, which are much higher than  $3.19 \times 10^4$  A/cm<sup>2</sup> and  $2.58 \times 10^3$  A/cm<sup>2</sup> of MgB<sub>2</sub> prepared using the non-milled powder. As the milling time further increases to 6 h, however,  $J_c$  decreases. The decrease of  $J_c$  for MgB<sub>2</sub> prepared using powder milled for 6 h is attributed to the presence of unreacted Mg and another phase, which was observed in the XRD patterns of Fig. 5. This result indicates that there is an optimum milling condition (optimum powder size) for the formation of a high  $J_c$  MgB<sub>2</sub>. A similar  $J_c$ - $B$  tendency with  $t$  was also observed at 20 K. The value of  $J_c$  at 5 K and 20 K, with a magnetic field of 2 T are presented in TABLE III.

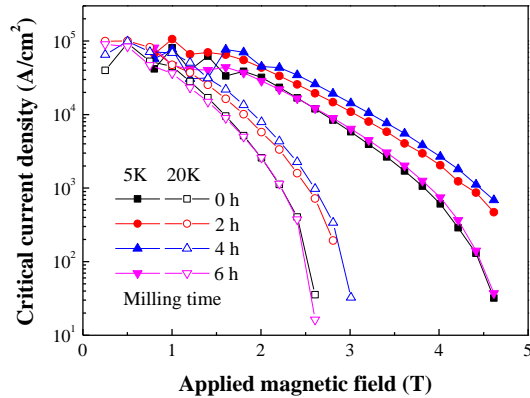


Fig. 8.  $J_c$ - $B$  curves at 5 K and 20 K of  $MgB_2$  prepared using the non-milled and  $(Mg+2B)$  powders milled for 2-6 h.

TABLE III

$J_c$  OF  $MgB_2$  AT 2 T, 5 K AND 20 K AS A FUNCTION OF MILLING TIME.

Milling time (h)	2 T, 5 K ( $A/cm^2$ )	2 T, 20 K ( $A/cm^2$ )
0	$3.19 \times 10^4$	$2.58 \times 10^3$
2	$4.34 \times 10^4$	$5.77 \times 10^3$
4	$4.49 \times 10^4$	$7.91 \times 10^3$
6	$2.87 \times 10^4$	$2.57 \times 10^3$

#### 4. CONCLUSIONS

This study presented the first experiment results for the cryomilling of Mg and B powders and the properties of  $MgB_2$  prepared using the milled powders. Mg and B powders were successfully milled together.  $MgB_2$  bulk superconductors were fabricated through the powder reaction process of  $(Mg+2B)$  milled for 0–6 h. It was found that the cryogenic milling process has the following advantages; (1) milling at low temperature suppressed the formation of MgO, which was often produced when using organic solvents or a Mg-O reaction, (2) Mg and B powders were simultaneously mixed uniformly and milled, (3) no carbon was incorporated with  $MgB_2$ , (4) the formation of  $MgB_2$  was promoted and (5) the grains size of  $MgB_2$  was effectively reduced, when the milling time was controlled properly. In this experiment, the optimum milling conditions for the fabrication of the high  $J_c$   $MgB_2$  bulk superconductors were 4 h period at 500 rpm. The values of  $J_c$  at 5 K and 20 K, with 2 T of  $MgB_2$  prepared using 4 h milled powder were  $4.49 \times 10^4 A/cm^2$  and  $7.91 \times 10^3 A/cm^2$ , respectively. When the milling time was increased to 6 h, however,  $J_c$  was decreased because the formation reaction of  $MgB_2$  was suppressed.

#### ACKNOWLEDGMENTS

This research was financially supported by the National Research Foundation Grant (NRF-2013M2A8A1035822) from Ministry of Science, ICT and Future Planning (MSIP) of Republic of Korea, and also partially supported by the Ministry of Trade, Industry and Energy (MOTIE)

and Korea Institute for Advancement of Technology (KIAT) through the Promoting Regional Specialized Industry.

#### REFERENCES

- [1] J. Nagamatsu, N. Nakagawa, T. Muranaka, Y. Zenitani and J. Akimitsu, "Superconductivity at 39 K in magnesium diboride," *Nature*, vol. 410, pp. 63, 2001.
- [2] A. V. Pan, S. Zhou, H. Liu and S. Dou, "Properties of superconducting  $MgB_2$  wires: *in situ* versus *ex situ* reaction technique," *Supercond. Sci. Technol.*, vol. 16, pp. 639-644, 2003.
- [3] B. A. Glowacki, M. Majoros, M. Vickers, J. E. Evetts, Y. Shi and I. Mcdougall, "Superconductivity of powder-in-tube  $MgB_2$  wires," *Supercond. Sci. Technol.*, vol. 14, pp. 193-199, 2001.
- [4] E. Martinez, L. A. Angurel and R. Navarro, "Study of Ag and Cu/ $MgB_2$  powder-in-tube composite wires fabricated by *in situ* reaction at low temperature," *Supercond. Sci. Technol.*, vol. 15, pp. 1043-1047, 2002.
- [5] B. H. Jun and C. J. Kim, "The effect of heat-treatment temperature on the superconducting properties of malic acid-doped  $MgB_2/Fe$  wire," *Supercond. Sci. Technol.*, vol. 20, pp. 980-985, 2007.
- [6] J. H. Kim, S. X. Dou, J. L. Wang, D. Q. Shi, X. Xu, M. S. A. Hossain, W. K. Yeoh, S. Choi and T. Kiyoshi, "The effects of sintering temperature on superconductivity in  $MgB_2/Fe$  wires," *Supercond. Sci. Technol.*, vol. 20, pp. 448-451, 2007.
- [7] A. Yamamoto, J. I. Shimoyama, S. Ueda, Y. Katsura, S. Horii and K. Kishio, "Improved critical current properties observed in  $MgB_2$  bulk synthesized by low-temperature solid-state reaction," *Supercond. Sci. Tehchnol.*, vol. 18, pp. 116-121, 2004.
- [8] C. J. Kim, J. H. Yi, B. H. Jun, B. Y. You, S. D. Park and K. N. Choo, "Reaction-induced pore formation and superconductivity in *in situ* processed  $MgB_2$  superconductors," *Physica C*, vol. 502, pp. 4-9, 2014.
- [9] G. S. Brady and H. R. Clauser, *Materials Handbook*, 12th ed., vol. 15. McGraw-Hill, 1956, pp. 104-105.
- [10] W. Goldacker, S. I. Schlachter, B. Obst and M. Eisterer, "*In-situ*  $MgB_2$  round wires with improved properties," *Supercond. Sci. Technol.*, vol. 17, pp. S490-495, 2004.
- [11] D. N. Kim, B. -H. Jun and S. -D. Park, "Effects of the size of Mg powder on the formation of  $MgB_2$  and the superconducting properties," *Prog. Supercond. Cryo., Korea*, vol. 18, pp. 9-14, 2016.
- [12] B. -H. Jun, N. -K. Kim, K. S. Tan and C. -J. Kim, "Enhanced critical current properties of *in situ* processed  $MgB_2$  wires using milled boron powder and low temperature solid-state reaction," *J. Alloys Compd.*, vol. 492, pp. 446-451, 2010.
- [13] X. Xu, J. H. Kim, W. K. Yeoh, Y. Zhang and S. X. Dou, "Improved  $J_c$  of  $MgB_2$  superconductor by ball milling using different media," *Supercond. Sci. Technol.*, vol. 19, pp. L47-50, 2006.
- [14] B. -H. Jun, Y. -J. Kim, K. S. Tan and C. -J. Kim, "Effective carbon incorporation in  $MgB_2$  by combining mechanical milling and the glycerin treatment of boron powder," *Supercond. Sci. Technol.*, vol. 21, pp. 105006, 2008.
- [15] J. Lee, F. Zhou, K. H. Jung, N. J. Kim and E. J. Lavernia, "Grain growth of nanocrystalline Ni powder prepared by cryomilling," *Metall. Mater. Trans.*, vol. 32A, pp. 3109-3115, 2001.
- [16] P. Scherrer, "Bestimmung der grösse und der inneren struktur von kolloidteilchen mittels röntgenstrahlen," *Nachr. Ges. Wiss. Göttingen*, vol. 26, pp. 98-100, 1918.
- [17] C. P. Bean, "Magnetization of high-field superconductors," *Rev. Mod. Phys.*, vol. 36, pp. 31-39, 1964.
- [18] C. J. Kim, H. G. Lee, D. Y. Wong and H. S. Shin, "Expansion of Bi-Sr-Ca-Cu-O pellets," *Mater. Sci. Eng. B*, pp. 501-505, 1989.
- [19] C. J. Kim, S.-J. L. Kang and D.-Y. Won, "Compact swelling in  $Bi_{1-x}Pb_xSr_2Ca_2Cu_{3.6}O_y$  during the formation of high- $T_c$  superconducting phase," *J. Am. Ceram. Soc.*, vol. 75, pp. 570-574, 1992.
- [20] J. H. Yi, K. T. Kim, B. H. Jun, J. M. Sohn, B. G. Kim, J. Joo and C. J. Kim, "Pore formation in *in situ* processed  $MgB_2$  superconductors," *Physica C*, vol. 469, pp.1192-1195, 2009.
- [21] C. F. Liu, G. Yan, S. J. Du, W. Xi, Y. Feng, P. X. Zhang, X. Z. Wu and L. Zhou, "Effect of heat-treatment temperatures on density and porosity in  $MgB_2$  superconductor," *Physica C*, vol. 386, pp. 603-606, 2003.

- [22] J. H. Kim, S. X. Dou, D. Q. Shi, M. Rindfleisch and M. Tomsic, "Study of MgO formation and structural defects in *in situ* processed MgB<sub>2</sub>/Fe wires," *Supercond. Sci. Technol.*, vol. 20, pp. 1026-1031, 2007.
- [23] A. Yamamoto, J. Shimoyama, S. Ueda, I. Iwayama, S. Horii and K. Kishio, "Effects of B<sub>4</sub>C doping on critical current properties of MgB<sub>2</sub> superconductor," *Supercond. Sci. Technol.*, vol. 18, pp. 1323-1328, 2005.